ISSN 0915-633X

NATIONAL INSTITUTE FOR FUSION SCIENCE

A Model of Sawtooth Based on the Transport Catastrophe

K. Itoh, S-I. Itoh and A. Fukuyama

(Received - Nov. 28, 1994)

NIFS-329 Dec. 1994

RESEARCH REPORT
NIFS Series

NAGOYA, JAPAN

A Model of Sawtooth
based on the Transport Catastrophe

K. Itoh*, S-I. Itoh† and A. Fukuyama**

* *National Institute for Fusion Science, Nagoya 464-01*

† *Research Institute for Applied Mechanics, Kyushu University 87, Kasuga 816*

** *Faculty of Engineering, Okayama University, Okayama 700*

Abstract

A new model of the sawtooth, which is not triggered by the m=1 helical mode, is proposed. The catastrophic change of the transport coefficient is predicted in the central region, where the safety factor q is lower than unity. The magnetic component in fluctuation increases as the plasma pressure increases. If the pressure gradient exceeds a certain threshold, a magnetic stochasticity sets in. The electron thermal conductivity can be enhanced by the factor of the ion-to-electron mass ratio, leading to the rapid flattening of the electron pressure profile. The enhanced transport coefficient also happens for ions. The increment of the transport associated with the strong magnetic perturbation continues until the ion pressure profile is flattened. Hysteresis behaviour of transport flux to the pressure gradient is obtained. The current profile is influenced by the enhanced current diffusivity from the same mechanism, but the change of the q profile remains small. Simple model equations which follow the dynamics are introduced. The dynamic solution of sawtooth crash is simulated.

Keywords: magnetic stochasticity, sawtooth, transport catastrophe, self-sustained turbulence, magnetic hill

1. Introduction

The sawtooth oscillation in tokamaks is characterized by the repetitive and rapid crash of the central electron temperature [1]. This phenomenon has been observed in all tokamaks and is considered to be a fundamental feature of the dynamics of the toroidal plasmas. The occurrence of the rapid crash and the resultant reformation of the plasma structure is intriguing from the view point of the structural development of the nonequilibrium systems.

The main efforts to understand the crash mechanism have been done by focusing to the dynamics of the m=1/n=1 helical mode (m and n are the poloidal and toroidal mode numbers, respectively.) The model by Kadomtsev [2], in which the m=1 island turns to the new magnetic axis after the reconnection process, has provided a starting point for understanding, followed by many numerical simulations. The fast crash in large tokamaks, however, has cast a problem to the reconnection model (see, e.g., [3]). More astonishing was the observation on the TEXTOR tokamak, which found the fact that the q value at the magnetic axis remains below unity [4]. In other words, the temperature profile shows fast flattening, but the magnetic structure is changed only little by the crash. This finding stimulated the theory which could simultaneously treat the full temperature crash and partial change of the magnetic structure. One theoretical approach to study the rapid grow of the m=1 mode is to investigate the effect of current diffusivity [5,6]. The role of the enhanced transport by the magnetic stochasticity in [5] is qualitatively supported by the detailed observation of crash on the WT-3 tokamak [7]. The feature of the subcritical turbulence was studied in analyzing the sawtooth cycle [8]. Although the sawtooth physics is progressed, a variety in sawtooth oscillations has been noticed experimentally. In some cases, the sawtooth is preceded by a long-lasting and saturated m=1 deformation, and the deformation persists after the crash as a long post cursors. In such sawtooth, the role of the m=1 mode may not be essential in causing the crash [9]. Some theory has been developed on sawtooth without describing the growth of the m=1 mode [10]. However, the dynamics of the crash was not necessarily clarified.

In this article we show a new model of the sawtooth which is independent of the growth of the m=1 mode. Recently, the theory of the anomalous transport and magnetic braiding has been developed by authors [11]. It was found that if the pressure gradient exceeds a certain threshold, the anomalous transport coefficient is subject to the catastrophic bifurcation. The hysteresis curve of the thermal conductivity was derived. The electron thermal conductivity χ_e can be enhanced by the factor of the ion-to-electron mass ratio, m_i/m_e, leading to the rapid flattening of the electron pressure profile. We apply this transport bifurcation to the model of sawtooth dynamics. In the core of the tokamak where the safety factor q is below unity, the averaged magnetic curvature is unfavourable: i.e., is the magnetic hill [12]. The critical pressure gradient for the transport bifurcation is calculated. The current profile is influenced by the enhanced current diffusivity. However, the change of the q profile remains small and the central q-value is below unity during the whole sawtooth period. This mechanism provides an understanding for the sawtooth which is not triggered by the burst of the m=1 helical mode.

2. L-mode and Transport Bifurcation

We consider the central region of tokamak where the q value is lower than unity. The averaged magnetic curvature is unfavourable, and the transport coefficient is governed by the interchange mode turbulence. The thermal conductivity in the L-mode was given as [13]

$$\chi_{e,i}^{L} = C \frac{(G_{0i} + G_{0e})^{3/2}}{s^2} \frac{c^2}{\omega_p^2} \frac{v_A}{R} \qquad (1)$$

where G_0 denotes the normalized equilibrium pressure gradient coupled to the magnetic curvature,

$$G_{0e,i} = (R/a)\Omega'(Rd\beta_{0e,i}/dr), \qquad (2)$$

$\Omega' = d\ln B/d\ln r$ and the superscript L indicates the L-mode. Notations: a and R are the minor and major radii, v_A is the Alfven velocity $v_A = B/\sqrt{\mu_0 m_i n_i}$, $s=r(dq/dr)q^{-2}$, $\beta_0 = 2\mu_0 p_0/B^2$. The averaged curvature is approximately given as $\Omega' = \varepsilon(1-1/q^2)$, $\varepsilon = r/R$. The one-point renormalization cannot determine the numerical coefficient of C, and the coefficient C is chosen by comparing χ to the experimental observations. According to [14], we choose C = 12. As the pressure increases, the perturbation starts to involve the magnetic component, and the characteristic wave length becomes longer.

When the pressure gradient exceeds a threshold as,

$$G_0 > G_c \approx 0.5\, s \tag{3}$$

($G_0 = G_{0i} + G_{0e}$ is the total normalized pressure gradient coupled to the bad magnetic curvature) the Chirikov condition for the magnetic component is satisfied. The jump to the large-scale, magnetic-turbulent state occurs, associated with self-sustained magnetic braiding . As a result of this magnetic stochasticity, the thermal conductivity is increased much. The result in [11] gives the relation $G_{0c} \approx 2.8C^{-2/3}s$, and the critical value of G_0 is given by Eq.(3) for C = 12. The explicit transport coefficients, in the case of magnetic braiding, are given as [11]

$$\chi_e^M = C^M \frac{\left(G_{0i} + G_{0e}\sqrt{m_e T_i/m_i T_e}\right)^{3/2}}{s^2} \frac{c^2}{\omega_p^2} \frac{v_A}{R} \frac{m_i T_e}{m_e T_i} \tag{4}$$

and

$$\chi_i^M = C^M \frac{\left(G_{0i} + G_{0e}\sqrt{m_e T_i/m_i T_e}\right)^{3/2}}{s^2} \frac{c^2}{\omega_p^2} \frac{v_A}{R} \sqrt{\frac{m_i T_e}{m_e T_i}} \tag{5}$$

The superscript M denotes the magnetic braiding. The numerical coefficient C^M in the magnetic turbulence may be different from that in the electric turbulence, C in Eq.(1),

but we here assume that $C = C^M$ for the simplicity. The electron thermal conductivity χ_e can be enhanced by the factor of the ion-to-electron mass ratio, m_i/m_e, leading to the rapid flattening of the electron pressure profile. The ion thermal conductivity χ_i is enhanced by the factor $\sqrt{m_i/m_e}$.

The state of increased transport coefficient, labeled by M-branch, disappears if the pressure gradient reaches the lower bound. The back transition to the L-mode is expected to occur at

$$G_1 = 1.7\beta_i \qquad (6)$$

($\beta_i = \mu_0 n_i T_i / B^2$). Figure 1 illustrates the hysteresis curve of the transport coefficient. The coefficient 1.7 comes from the factor $C^{-2/3}$ which was neglected in Ref.[11].

3. Dynamical Model of Sawtooth

The bifurcation at $G_0 = G_c$ causes the rapid crash at the critical pressure gradient. On the other hand the bifurcation at $G_0 = G_1$, however, initiates the pile up of the pressure gradient. The hysteresis curve of the transport coefficient gives rise to the limit cycle behaviour with the transport time scale. The temporal evolution of the system is modelled, and is studied by focusing on the behaviour of the transport coefficient and the pressure gradient.

3.1 Dynamical Model

3.1.1 Connection Formula of Transport Coefficient and Its Dynamical Change

In the following analysis, the transport coefficient is represented by the ion viscosity μ. It is shown that the ion Prandtl number, χ_i/μ, is close to unity in the electrostatic limit [15] as well as in the magnetic braiding limit [16]. The ratio $\zeta = \chi_e/\chi_i$ is newly introduced as well. By using μ and ζ we here employ the simplified relations

$$\chi_i = \mu \qquad (7\text{-}1)$$

and

$$\chi_e = \zeta\mu. \tag{7-2}$$

In the electric turbulence limit, the relation $\zeta = 1$ holds. In the limit of magnetic turbulence with the complete braiding, we have $\zeta = \sqrt{m_i T_e / m_e T_i}$. The magnetic stochasticity occurs when the turbulence level exceeds the Chirikov criterion. The stochasticity condition is usually discussed in terms of the perturbation amplitude. In the strong turbulence limit, the relation $\mu \propto \phi \propto \tilde{B}$ holds (ϕ and $\tilde{B}$ being the fluctuation amplitudes), and we here represent the stochasticity condition in terms of the transport coefficient. We introduce a critical value μ_c, i.e., μ_c is the value of μ at which the magnetic stochasticity occurs. Then an interpolation formula for ζ is employed as

$$\zeta\left(\equiv \frac{\chi_e}{\chi_i}\right) = 1 + \sqrt{\frac{m_i T_e}{m_e T_i}}\left(1 - \frac{\mu_c}{\mu}\right)\Theta(\mu - \mu_c) \tag{8}$$

by simulating the case of the magnetic braiding as

$$\zeta = 1 + \sqrt{\frac{m_i T_e}{m_e T_i}}\left(1 - \frac{\tilde{B}_c}{\tilde{B}}\right)\Theta(\tilde{B} - \tilde{B}_c) \tag{8'}$$

where Θ is a Heaviside function. The Heaviside function represents the onset of stochasticity . The transport coefficient for the process of the transition from L-mode to the M-mode (and vice versa) is smoothly connected by Eq.(8).

The dynamical variation of the transport coefficient, in accordance with the turbulence level, is modelled. The coefficient changes from that in the stationary states, with the growth rate γas

$$d\mu/dt = \gamma\,\mu \tag{9}$$

and

$$\gamma\tau_{Ap} = \sqrt{G_0}\,(1 - \mu/\mu_s) \tag{10}$$

The nonlinear growth and damping are modelled to a form of $(1-\mu/\mu_s)$. This form is studied and is confirmed by the analysis by use of the renormalization of turbulence [13,17]. In Eq.(10), μ_s indicates the saturation amplitude of fluctuation as well as the value of μ at the saturation level. For the magnetic turbulence, noting Eqs.(1), (4) and (5), we have

$$\chi_{e\,s} = \chi^{L}\left(\frac{G_{0i}+ G_{0e}/\zeta}{G_{0i}+ G_{0e}}\right)^{3/2}\zeta^2 \tag{11}$$

and

$$\mu_s = \chi_{i\,s} = \chi^{L}\left(\frac{G_{0i}+ G_{0e}/\zeta}{G_{0i}+ G_{0e}}\right)^{3/2}\zeta \tag{12}$$

which recover the electric turbulence limit (ζ=1) and the magnetic turbulence limit ($\zeta=\sqrt{m_iT_e/m_eT_i}$), i. e., $\mu_s = \chi^L$ in the L-branch and $\mu_s = \chi_i^M$ and $\chi_e = \chi_e^M$ in the M-branch. For the reference, the values of μ_s are plotted against G_0 in Fig.1.

3.1.2 Evolution of Plasma Profile

The increment of the transport coefficient associated with the strong magnetic perturbation continues until the total pressure gradient is reduced, so that $G_0 < G_1$ is satisfied. The development of the pressure gradient is given as

$$\frac{\partial p_0}{\partial t} = P + \nabla\cdot\chi\,\nabla p_0 \tag{13}$$

where P is the heating power density per unit volume. We here consider the model equations of the onset of the crash for the pressure gradients of ions and electrons. Introducing an energy confinement time in the core region of the L-branch,

$$\tau_{Ec} \approx r_c^2/\chi^L, \tag{14}$$

(r_c is the radius at which the crash happens), the operator $\nabla\cdot\chi\nabla$ can be evaluated by the quantity $-(\chi/\chi_L)(1/\tau_{Ec})$ for each electron and ion component. Then Eq.(13) is simply modelled to the zero-dimensional equation as

$$\frac{dG_{0i}}{dt} = \frac{1}{\tau_{Ec}}\left(G_{L\,i} - \frac{\mu}{\chi_i^L}G_{0i}\right) \tag{15}$$

for the ion component and

$$\frac{dG_{0e}}{dt} = \frac{1}{\tau_{Ec}}\left(G_{Le} - \frac{\mu\zeta}{\chi_e^L}G_{0e}\right) \tag{16}$$

for the electron component. The heating power P is rewritten in terms of the equilibrium pressure gradient G_L which would be realized in the confinement of the L-branch, $\mu = \chi_i$ and $\zeta = 1$. We assume that the heating power is affected little by the onset of crash. The change of the current profile is governed by the current diffusivity, λ, which is given by $\lambda = \chi_e(c/a\omega_p)^2$.

3.2 Sawtooth

3.2.1 Temporal Evolution

We analyze the developments of the thermal conductivity and the pressure gradients by use of the zero dimensional model. Equations (9), (15) and (16), together with Eqs.(8), (10), (11) and (12), are solved, and the temporal evolution of (μ, ζ, G_{0i} and G_{0e}) is followed by taking the parameter τ_E/τ_{Ap} and G_L. We employ the condition $T_e = T_i$ and $G_{Li} = G_{Le}$ for the simplicity. In the following study, parameters τ_E/τ_{Ap} and G_L are assumed to be constant in time. The heating power (e.g., Ohmic heating power) density can change after the crash, owing to the modification of the temperature profile. However, in the central region of the plasma, the relative change of the temperature is much weaker than its gradient.

Figure 2 illustrates the dynamic behaviour at the crash. We choose the parameters $s = 0.16$, $\beta_i = 0.25\%$, $G_L/G_c = 1.1$ and $\tau_{Ec}/\tau_{Ap} = 5000$. The mass ratio is taken as $m_i/m_e = 1836$. At the time $t = 0$, the pressure gradient reaches to the critical condition, Eq.(3), i.e., the Chirikov condition for the magnetic component of fluctuations. The stochasticity, which indicates the magnetic braiding, is switched on, and the ratio of the electron thermal conductivity to that of ions starts to increase in the time scale of $10\tau_{Ap}$. The thermal conductivity of electrons is enhanced by the factor of $O(m_i/m_e)$, and the electron pressure crashes in the time scale of $O(\tau_E m_e/m_i)$. In the calculation, the maximum enhancement of χ_e to the initial value is about 500. This reduction from m_i/m_e is due to the fact that the electron pressure gradient is reduced when the stochasticity is fully developed. The ion conductivity is also enhanced, and the ion pressure gradient is subject to the crash as well. The bursts of the turbulence and the anomalous transport coefficient continue until the total pressure is reduced to the level of Eq.(6). Therefore the crash time of ion pressure gradient, $O(\tau_{Ec}\sqrt{m_e/m_i})$, determines the duration of the bursts. The duration time is a few hundred times of τ_{Ap}. After the enhanced turbulent state terminates, the plasma pressure starts to increase, following to the L-mode confinement law. When the pressure gradient reaches the critical value, the crash happens again. The slow build up and fast crash occur in a repetitive manner. This sequence is seen as a sawtooth.

This theory also predicts the associated change of the current profile during the crash. The current diffusivity λ is estimated to be $\lambda = \chi_e(c/\omega_p)^2$. This indicates that the rate of the change of current gradient inside the radius r_c, τ_j, compared to that of the ion pressure, τ_i, is given as

$$\tau_j \approx (r_c\omega_p/c)^2 \sqrt{m_e/m_i}\, \tau_i. \qquad (17)$$

In large devices, the values of $r_c\omega_p/c$ reaches to 50 - 100. This suggests that the time for the current diffusion is about 50 -100 times longer than that for the ion pressure gradient, even in the magnetic turbulent state. The change of the current profile remains

small during the crash, because the burst duration is approximately given by τ_i. The theory predicts that the electron temperature gradient crashes almost completely but, during this period, the relative change of q profile remains to be a few per cent. In a smaller machines, the current diffusion time becomes closer to the ion-pressure diffusion time.

Let us estimate the typical mode number of the fluctuations. The typical mode number changes from m_0, which is a typical mode number at $G_0 = G_c$, to

$$m = r_c k_\theta = m_0 \left(\frac{\mu}{\chi_e}\right)^{1/2} \left(\frac{G_{0i} + G_{0e}\chi_i/\chi_e}{G_c}\right)^{-1/2} \qquad (18\text{-}1)$$

The expression of m_0 is given as [13]

$$m_0 = \frac{r_c \omega_p}{c} \sqrt{s} \qquad (18\text{-}2)$$

Rough estimate gives the mode number $m = r_c k_\theta$ being about a few tens to 100 in the L-mode and around 10 in the M-branch. Figure 3 illustrates the change of the typical mode number at the sawtooth crash in this theory.

3.2.2 Spatial Location

The radial location, where the crash starts in the first beginning, is estimated from Eq.(3) It exists in between the axis and the q=1 rational surface. The energy balance equation Eq.(13), in the stationary state, with Eq.(1) gives the proportionality relation near the axis as

$$-\chi \nabla p_0 \simeq \frac{r}{2} P_0 \qquad (19)$$

where P_0 is the heating power density at the axis. The χ-value in the L-mode is written as

$$\chi = \xi \frac{1}{s^2} (\Omega' p_0')^{3/2} \tag{20}$$

where $\xi = C(c/\omega_p)^2(2\mu_0 v_A R/aB^2)$ is taken to be a constant. From Eqs.(19) and (20), we have an estimate for the pressure gradient

$$\frac{(\Omega')^{3/2}}{s^2}(p_0')^{5/2} = \xi P_0 r \tag{21}$$

From Eq.(21), we have the radial dependence of G_0 as

$$G_0 = \left(\xi \frac{R^2}{a^2} P_0\right)^{2/5} r^{2/5} s^{4/5} (\Omega')^{2/5} \tag{22}$$

in the L-branch. The ratio of G_0 to G_c (Eq.(3)) has the dependence as

$$\frac{G_0}{G_c} = \left(\xi \frac{R^2}{a^2} P_0\right)^{2/5} r^{2/5} s^{-1/5} (\Omega')^{2/5} \tag{23}$$

We see that the function

$$f(r) = r^{2/5} s^{-1/5} (\Omega')^{2/5} \tag{24}$$

describes the radial form of the ratio G_0/G_c. The function f(r) vanishes at r = 0 and r = r_1, (r_1 being the m = 1 mode rational surface, $q(r_1) = 1$, where the magnetic hill vanishes) and takes the maximum in between.

For a simplified model, $q(r) = q_0 + (1-q_0)(r/r_1)^2$ and $\Omega' = (r/R)(1-q^{-2})$, the function f(r) takes the maximum value $(8r_1/27qR)^{2/5}(1-q_0)^{2/5}$ at $r = r_c$ and r_c is given as

$$r_c = r_1/\sqrt{3}. \tag{25}$$

The crash most easily takes place near the region of $r/r_1 = 0.6$.

This type of the crash happens when the condition Eq.(3) is satisfied at some plasma radius. As the central q value become smaller, this type of sawtooth crash more easily occurs. This is because the critical condition of the pressure gradient is a *decreasing* function of $1-q_0$. The condition Eq.(3) is compared to the pressure gradient limit against the linear m = 1 ideal MHD instability [3, 18]. The critical pressure gradient is an increasing function of $1- q_0$ in the case of the linear ideal MHD mode. For the parabolic profiles of the current and pressure, the critical condition was obtained from linear MHD theory as $\beta_{p1} \geq \beta_{pc}(\mathrm{MHD}) \simeq \sqrt{13}/12$, where β_{p1} is the averaged gradient of poloidal β-value inside the q = 1 surface and is defined as

$$\beta_{p1} = \frac{R^2}{r_1^4}\int_0^{r_1} \beta_0' r^2 dr$$

As q_0 approaches to unity, $\beta_{pc}(\mathrm{MHD})$ goes to zero. Equation (3) gives an estimate $\beta_{pc} \simeq R/8r_1$ which is close to unity. The criterion is slightly higher than that from the ideal MHD theory, $\beta_{pc}(\mathrm{MHD})$, although the absolute value in the coefficient of Eq.(3) contains uncertainty due to the analytic approximations in [11]. There is an experimental observation which suggests that the pressure gradient of the core plasma is in the range of the ideal MHD beat limit at the onset the sawtooth collapse [19]. The critical pressure gradient in this article may be related to this observation. We see that when q_0 is around 0.8, this type of crash could occur in the central region of the plasma.

4. Summary and Discussion

In summary, we have proposed a new mechanism of the fast crash of the pressure gradient in the central region of tokamak plasma with $q_0 < 1$. The mechanism leading to the fast crash is the onset of the magnetic stochasticity due to the magnetic component of fluctuations. The fluctuations are considered to be the origin of the

anomalous transport in the L-mode. The electron and thermal conductivities are increased by factors of m_i/m_e and $\sqrt{m_i/m_e}$, respectively. The strong increment of the transport, associated with the magnetic fluctuations of the lower mode numbers, continues until the ion pressure gradient is suppressed so that the total plasma pressure is below the critical value. For typical plasma parameters of present day experiments, the crash time of the electron pressure is about a few ten times τ_{Ap}. The duration of the burst is a few hundred times τ_{Ap}. The q profile is also modified by the transport catastrophe, but the relative change remains of the order of a few per cent. The crash occurs in the beginning near the region $r/r_1 \approx 0.6$. This model provides an understanding for the sawtooth crash which is not triggered by the explosive growth of the m = 1 mode.

We here note on the period of the sawtooth oscillation of this kind. The crash happens again if the pressure gradient recovers to the critical pressure gradient. This suggests that, if other parameters are unchanged, the period becomes shorter when the central heating power density increases. Not all the sawtooth oscillation in experiments obeys this rule. The sawtooth which is driven by the mechanism in this article could be distinguished from other kinds of sawtooth by studying the dependence of the oscillation period on the central heating power.

The analysis on the transport bifurcation provides a new physics picture of the dynamics near the limit of pressure gradient (i.e., so called β-limit) The fluctuation level and transport coefficient behave like the case of subcritical turbulence, rather than the pitch fork bifurcation of the usual linear instability. This method could be applied to the other cases of the beta limiting phenomena. The analysis on the phenomena such as Type-I ELM [20] is performed and will be reported.

Acknowledgements

This paper is dedicated to Prof. B. Coppi on occasion of his sixtieth birthday. Authors acknowledge collaboration and discussion with Prof. A. J. Lichtenberg on the role of the stochasticity. They are grateful to the discussion on the physics of sawtooth with Drs. S. Tsuji, M. Azumi, M. Yagi, J. Wesson, W. Stodiek, D. J. Campbell, H. Soltwisch. This work is partly supported by the Grant-in-Aid for Scientific Research of Ministry of Education Japan and by the collaboration program of Advanced Fusion Research Center of Kyushu University.

References

[1] von Goeler S, Stodiek W and Sauthoff N 1974 *Phys. Rev. Lett.* **33** 1201.

[2] Kadomtsev B B 1975 *Phys. Plasmy* **1** 710 [*Sov. J. Plasma Phys.* **1** 389 (1976)]. For the m=1 instability, see Coppi B, Galvao R, Pellat R, Rosenbluth M N, and Rutherford P H 1976 *Sov. J. Plasma Phys.* **2** 533.

[3] Wesson J 1987 in *Theory of Fusion Plasmas* (Proc. International School of Plasma Physics, Varenna) (ed. A Bondeson, E. Sindoni, F. Troyon, Editrice Compositori, Bologna) 253.

[4] Soltwisch H, Stodiek W, Manickam J and Schluter J 1987 in *Plasma Physics And Controlled Nuclear Fusion Research 1986* (IAEA, Vienna) Vol.1 263.

[5] Lichtenberg A J, Itoh K, Itoh S-I, Fukuyama A 1992 *Nucl. Fusion* **32** 495.

[6] Wesson J 1991 in *Plasma Physics And Controlled Nuclear Fusion Research 1990* (IAEA, Vienna) Vol. 2 p.79.
Aydemir A Y 1992 *Phys. Fluids* B **4** 3469.
Biskamp D and Drake J F 1994 *Phys. Rev. Lett.* **73** 971.

[7] Hanada K 1994 *J. Phys. Soc. Jpn.* **63** 967.

[8] Fukuyama A, Itoh K, Itoh S-I, Tsuji S and Lichtenberg A J 1993 in *Plasma Physics And Controlled Nuclear Fusion Research 1992* (IAEA, Vienna) Vol.2, p.363.

[9] Snipes J A and Gentle K W 1986 *Nucl. Fusion* **26** 1507.

[10] Gimblett C G and Hastie R J 1994 'Computational Model for Sawtooth Crash' (Research Report AEA FUS 260, Culham Laboratory).

[11] Itoh K, Fukuyama A, Itoh S-I, Yagi M and Azumi M 1994 'Self-Sustained Magnetic Braiding in Toroidal Plasmas' (Research Report NIFS-288, National Institute for Fusion Science), submitted to *Phys. Rev. Lett.*

[12] Miyamoto K 1987 '*Plasma Physics for Nuclear Fusion*' (2nd ed., Iwanami, Tokyo) Chapter 9.4.

[13] Itoh K, Itoh S-I and Fukuyama A 1992 *Phys. Rev. Lett.* **69** 1050.

Itoh K, Itoh S-I, Fukuyama A, Yagi M and Azumi M 1994 *Plasma Phys. Contr. Fusion* **36** 1501.

[14] Fukuyama A, Itoh K, Itoh S-I, Yagi M and Azumi M 1994 *Plasma Phys. Contr. Fusion* **36** 1385.

[15] Itoh K, Itoh S-I, Fukuyama A, Yagi M and Azumi M 1993 *J. Phys. Soc. Jpn.* **62** 4269.

[16] Lichtenberg A J, Itoh K, Itoh S-I, Fukuyama A 1992 *Nucl. Fusion* **32** 495.

[17] Yagi M, Itoh K, Itoh S-I, Fukuyama A and Azumi M 1993 *Phys. Fluids B* **5** 3702.

[18] Bussac M N, Pellat R, Edery D and Soule J L 1975 *Phys. Rev. Lett.* **35** 1638.

[19] Stodiek W 1992 private communications.

[20] Burrell K H et al 1989 *Plasma Phys. Contr. Fusion* **31** 1649.

Zohm H, Wagner F, Endler M, Gernhardt J, Holzhauer E, Kerner W, Mertens V 1992 *Nucl. Fusion* **32** 489.

Figure Captions

Fig. 1 Transport coefficient as a function of the pressure gradient. χ vs G_0 is shown. The electron pressure gradient and ion pressure gradient are taken equal. At critical values of gradient, G_c and G_1, the bifurcation takes place. The jump from L- to M-branch and that from M- to L-branch occur at $G_0 = G_c$ and $G_0 = G_1$, respectively.

Fig. 2 Temporal evolution at the crash. The normalized pressure gradient (top), the ion thermal conductivity (middle) and the ratio of χ_e/χ_i (bottom) are shown. In (a), the change during the whole burst is shown. At time $t = 0$, the stochasticity onsets, and the crash starts. The magnetic braiding terminates at $t/\tau_{Ap} \approx 300$, and the pressure gradient starts to increase again. The expanded view near the onset of the crash is shown in (b). (Parameters are: $s = 0.16$, $\beta_i = 0.25\%$, $\tau_{Ec}/\tau_{Ap} = 5000$, $T_e = T_i$, and $G_{Li} = G_{Le} = 0.55G_c$).

Fig.3 Change of the mode number m of the fluctuations at the sawtooth crash. The mode number decreases rapidly associated with the increment of the transport coefficient. When the stochasticity terminates, the mode number becomes larger than the initial value, owing to the reduced pressure gradient after the crash. (a) and (b) corresponds to those in Fig.2, respectively. Normalizing mode number is given as $m_0 = \sqrt{s}(r_c\omega_p/c)$.

Fig. 1

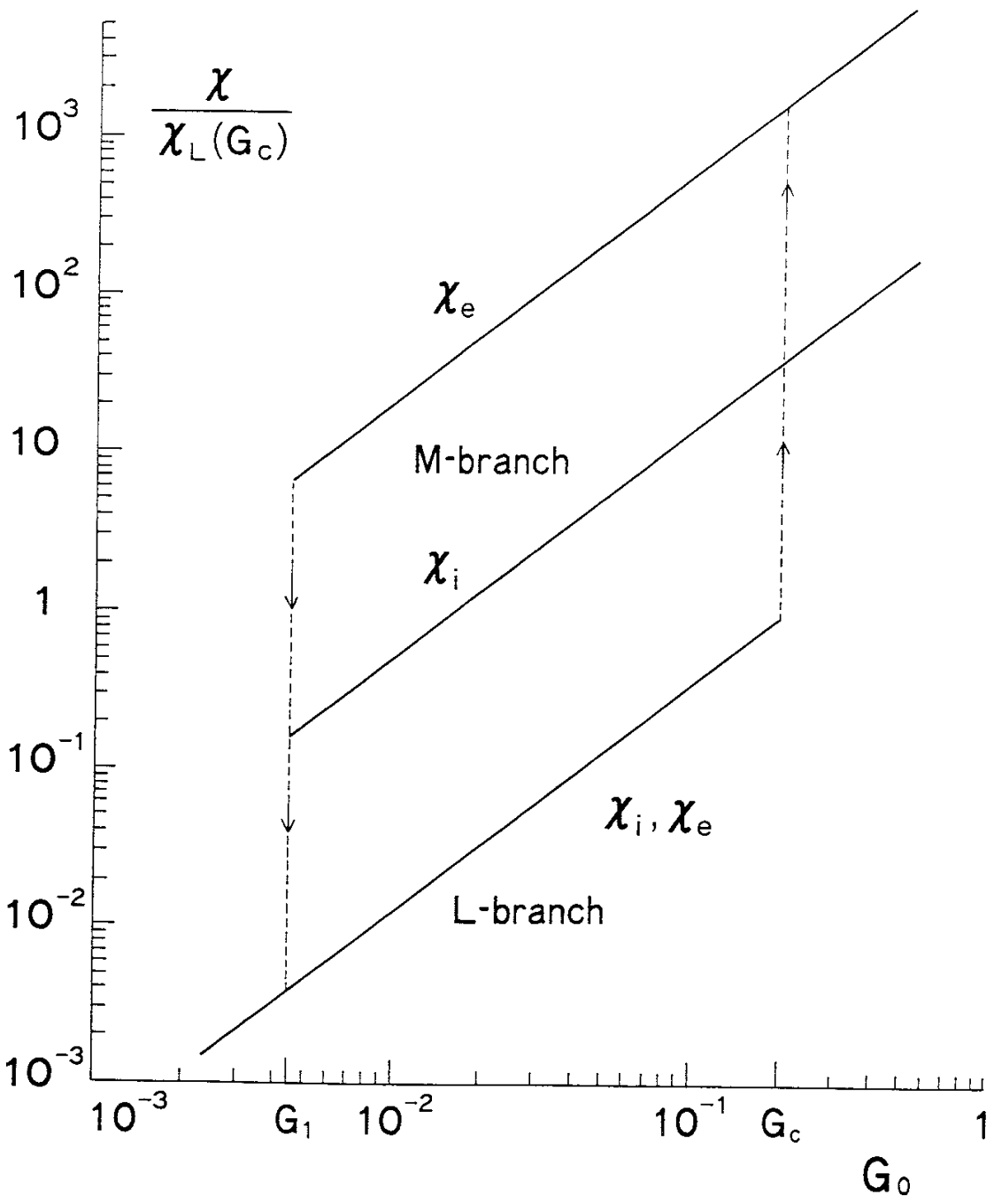
$\frac{\chi}{\chi_L(G_c)}$
10^3
10^2
10
1
10^{-1}
10^{-2}
10^{-3}
χ_e
M-branch
χ_i
χ_i, χ_e
L-branch
10^{-3}
G_1
10^{-2}
10^{-1}
G_c
1
G_0

Fig. 2

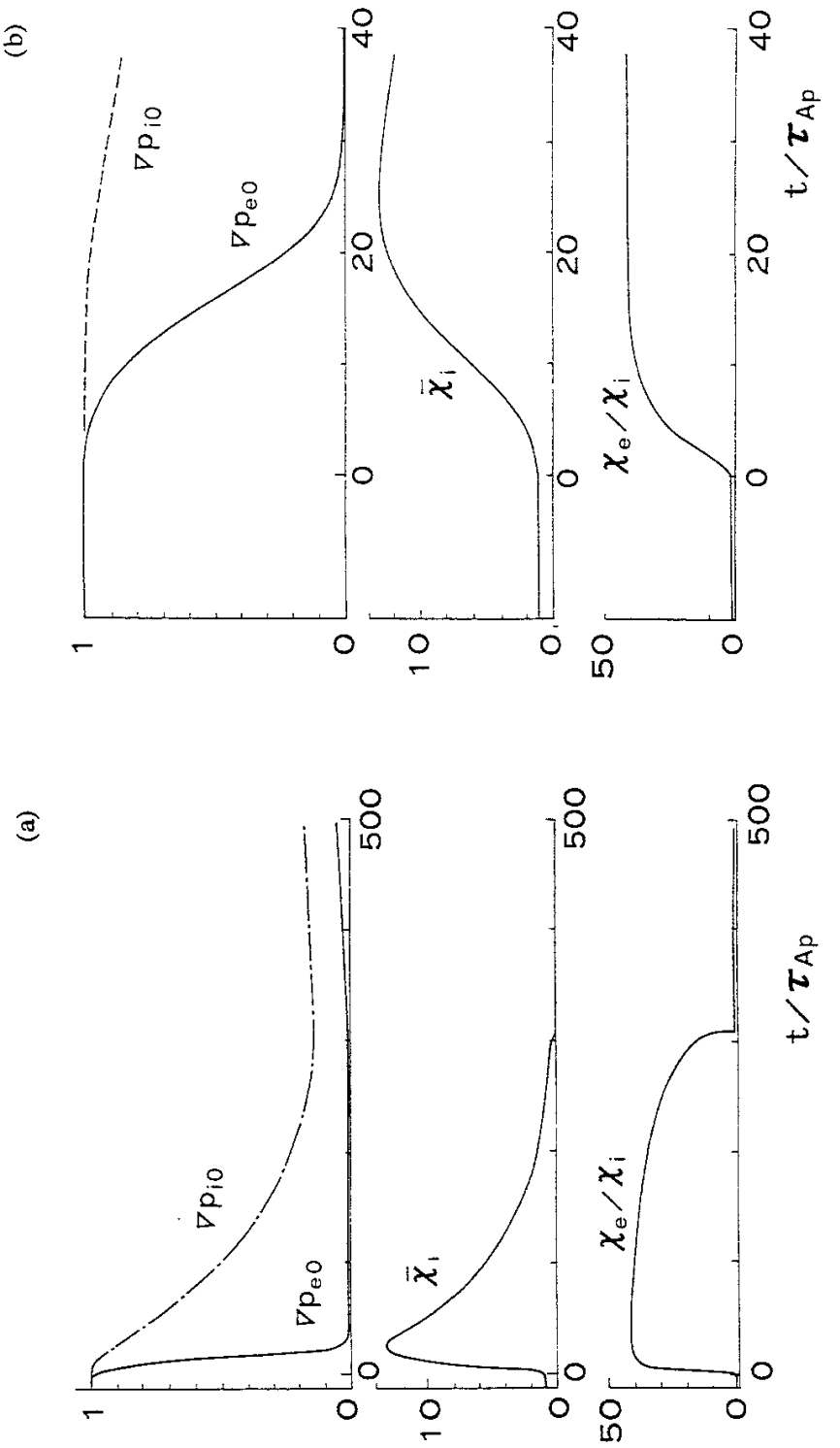
(a)
(b)
∇p_{i0}
∇p_{e0}
$\bar{\chi}_i$
χ_e / χ_i
1
0
10
50
0
20
40
500
t / τ_{Ap}

Fig.3

(a)

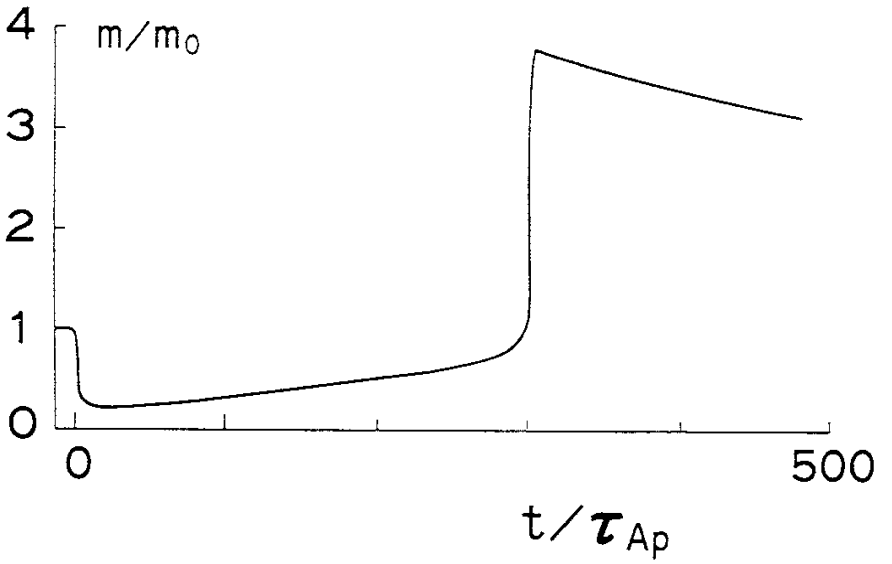

(b)

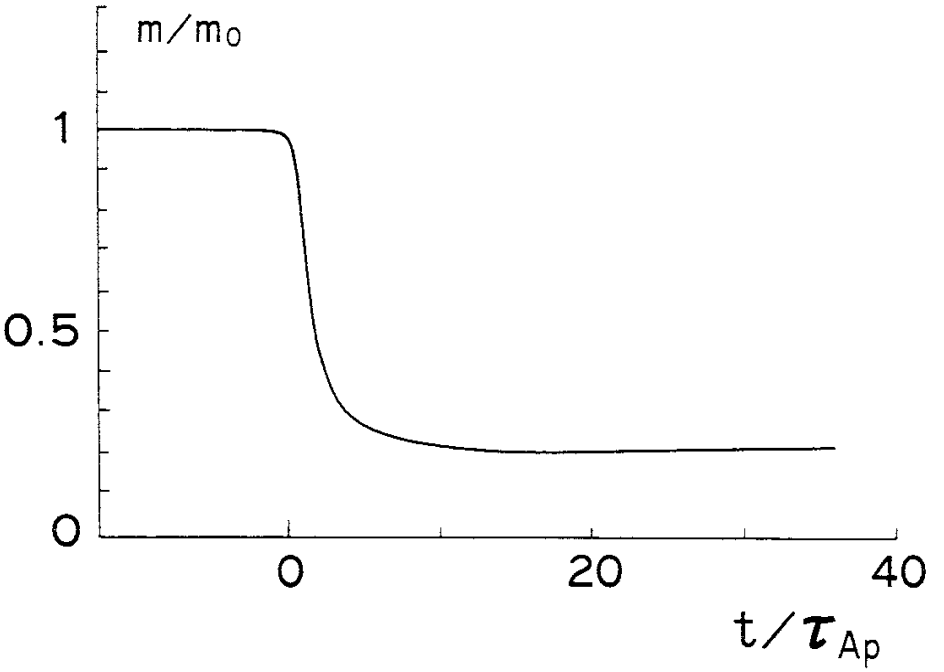

Recent Issues of NIFS Series

NIFS-289 Y. Nejoh,
Relativistic Effects on Large Amplitude Nonlinear Langmuir Waves in a Two-Fluid Plasma; July 1994

NIFS-290 N. Ohyabu, A. Komori, K. Akaishi, N. Inoue, Y. Kubota, A.I. Livshit, N. Noda, A. Sagara, H. Suzuki, T. Watanabe, O. Motojima, M. Fujiwara, A. Iiyoshi,
Innovative Divertor Concepts for LHD; July 1994

NIFS-291 H. Idei, K. Ida, H. Sanuki, S. Kubo, H. Yamada, H. Iguchi, S. Morita, S. Okamura, R. Akiyama, H. Arimoto, K. Matsuoka, K. Nishimura, K. Ohkubo, C. Takahashi, Y. Takita, K. Toi, K. Tsumori and I. Yamada,
Formation of Positive Radial Electric Field by Electron Cyclotron Heating in Compact Helical System; July 1994

NIFS-292 N. Noda, A. Sagara, H. Yamada, Y. Kubota, N. Inoue, K. Akaishi, O. Motojima, K. Iwamoto, M. Hashiba, I. Fujita, T. Hino, T. Yamashina, K. Okazaki, J. Rice, M. Yamage, H. Toyoda and H. Sugai,
Boronization Study for Application to Large Helical Device; July 1994

NIFS-293 Y. Ueda, T. Tanabe, V. Philipps, L. Könen, A. Pospieszczyk, U. Samm, B. Schweer, B. Unterberg, M. Wada, N. Hawkes and N. Noda,
Effects of Impurities Released from High Z Test Limiter on Plasma Performance in TEXTOR; July. 1994

NIFS-294 K. Akaishi, Y. Kubota, K. Ezaki and O. Motojima,
Experimental Study on Scaling Law of Outgassing Rate with A Pumping Parameter, Aug. 1994

NIFS-295 S. Bazdenkov, T. Sato, R. Horiuchi, K. Watanabe,
Magnetic Mirror Effect as a Trigger of Collisionless Magnetic Reconnection, Aug. 1994

NIFS-296 K. Itoh, M. Yagi, S.-I. Itoh, A. Fukuyama, H. Sanuki, M. Azumi,
Anomalous Transport Theory for Toroidal Helical Plasmas,
Aug. 1994 (IAEA-CN-60/D-III-3)

NIFS-297 J. Yamamoto, O. Motojima, T. Mito, K. Takahata, N. Yanagi, S. Yamada, H. Chikaraishi, S. Imagawa, A. Iwamoto, H. Kaneko, A. Nishimura, S. Satoh, T. Satow, H. Tamura, S. Yamaguchi, K. Yamazaki, M. Fujiwara, A. Iiyoshi and LHD group,
New Evaluation Method of Superconductor Characteristics for Realizing the Large Helical Device; Aug. 1994 (IAEA-CN-60/F-P-3)

NIFS-298 A. Komori, N. Ohyabu, T. Watanabe, H. Suzuki, A. Sagara, N. Noda, K. Akaishi, N. Inoue, Y. Kubota, O Motojima, M. Fujiwara and A. Iiyoshi,
Local Island Divertor Concept for LHD; Aug. 1994 (IAEA-CN-60/F-P-4)

NIFS-299 K. Toi, T. Morisaki, S. Sakakibara, A. Ejiri, H. Yamada, S. Morita, K. Tanaka, N. Nakajima, S. Okamura, H. Iguchi, K. Ida, K. Tsumori, S. Ohdachi, K. Nishimura, K. Matsuoka, J. Xu, I. Yamada, T. Minami, K. Narihara, R. Akiyama, A. Ando, H. Arimoto, A. Fujisawa, M. Fujiwara, H. Idei, O. Kaneko, K. Kawahata, A. Komori, S. Kubo, R. Kumazawa, T. Ozaki, A. Sagara, C. Takahashi, Y. Takita and T. Watari, *Impact of Rotational-Transform Profile Control on Plasma Confinement and Stability in CHS*; Aug. 1994 (IAEA-CN-60/A6/C-P-3)

NIFS-300 H. Sugama and W. Horton, *Dynamical Model of Pressure-Gradient-Driven Turbulence and Shear Flow Generation in L-H Transition;* Aug. 1994 (IAEA/CN-60/D-P-I-11)

NIFS-301 Y. Hamada, A. Nishizawa, Y. Kawasumi, K.N. Sato, H. Sakakita, R. Liang, K. Kawahata, A. Ejiri, K. Narihara, K. Sato, T. Seki, K. Toi, K. Itoh, H. Iguchi, A. Fujisawa, K. Adachi, S. Hidekuma, S. Hirokura, K. Ida, M. Kojima, J. Koog, R. Kumazawa, H. Kuramoto, T. Minami, I. Negi, S. Ohdachi, M. Sasao, T. Tsuzuki, J. Xu, I. Yamada, T. Watari, *Study of Turbulence and Plasma Potential in JIPP T-IIU Tokamak*; Aug. 1994 (IAEA/CN-60/A-2-III-5)

NIFS-302 K. Nishimura, R. Kumazawa, T. Mutoh, T. Watari, T. Seki, A. Ando, S. Masuda, F. Shinpo, S. Murakami, S. Okamura, H. Yamada, K. Matsuoka, S. Morita, T. Ozaki, K. Ida, H. Iguchi, I. Yamada, A. Ejiri, H. Idei, S. Muto, K. Tanaka, J. Xu, R. Akiyama, H. Arimoto, M. Isobe, M. Iwase, O. Kaneko, S. Kubo, T. Kawamoto, A. Lazaros, T. Morisaki, S. Sakakibara, Y. Takita, C. Takahashi and K. Tsumori, *ICRF Heating in CHS*; Sep. 1994 (IAEA-CN-60/A-6-I-4)

NIFS-303 S. Okamura, K. Matsuoka, K. Nishimura, K. Tsumori, R. Akiyama, S. Sakakibara, H. Yamada, S. Morita, T. Morisaki, N. Nakajima, K. Tanaka, J. Xu, K. Ida, H. Iguchi, A. Lazaros, T. Ozaki, H. Arimoto, A. Ejiri, M. Fujiwara, H. Idei, A. Iiyoshi, O, Kaneko, K. Kawahata, T. Kawamoto, S. Kubo, T. Kuroda, O. Motojima, V.D. Pustovitov, A. Sagara, C. Takahashi, K. Toi and I. Yamada, *High Beta Experiments in CHS*; Sep. 1994 (IAEA-CN-60/A-2-IV-3)

NIFS-304 K. Ida, H. Idei, H. Sanuki, K. Itoh, J. Xu, S. Hidekuma, K. Kondo, A. Sahara, H. Zushi, S.-I. Itoh, A. Fukuyama, K. Adati, R. Akiyama, S. Bessho, A. Ejiri, A. Fujisawa, M. Fujiwara, Y. Hamada, S. Hirokura, H. Iguchi, O. Kaneko, K. Kawahata, Y. Kawasumi, M. Kojima, S. Kubo, H. Kuramoto, A. Lazaros, R. Liang, K. Matsuoka, T. Minami, T. Mizuuchi, T. Morisaki, S. Morita, K. Nagasaki, K. Narihara, K. Nishimura, A. Nishizawa, T. Obiki, H. Okada, S. Okamura, T. Ozaki, S. Sakakibara, H. Sakakita, A. Sagara, F. Sano, M. Sasao, K. Sato, K.N. Sato, T. Saeki, S. Sudo, C. Takahashi, K. Tanaka, K. Tsumori, H.Yamada, I. Yamada, Y. Takita, T. Tuzuki, K. Toi and T. Watari, *Control of Radial Electric Field in Torus Plasma;* Sep. 1994 (IAEA-CN-60/A-2-IV-2)

NIFS-305 T. Hayashi, T. Sato, N. Nakajima, K. Ichiguchi, P. Merkel, J. Nührenberg, U. Schwenn, H. Gardner, A. Bhattacharjee and C.C.Hegna, *Behavior of Magnetic Islands in 3D MHD Equilibria of Helical Devices*; Sep. 1994 (IAEA-CN-60/D-2-II-4)

NIFS-306 S. Murakami, M. Okamoto, N. Nakajima, K.Y. Watanabe, T. Watari, T. Mutoh, R. Kumazawa and T. Seki, *Monte Carlo Simulation for ICRF Heating in Heliotron/Torsatrons*; Sep. 1994 (IAEA-CN-60/D-P-I-14)

NIFS-307 Y. Takeiri, A. Ando, O. Kaneko, Y. Oka, K. Tsumori, R. Akiyama, E. Asano, T. Kawamoto, T. Kuroda, M. Tanaka and H. Kawakami, *Development of an Intense Negative Hydrogen Ion Source with a Wide-Range of External Magnetic Filter Field*; Sep. 1994

NIFS-308 T. Hayashi, T. Sato, H.J. Gardner and J.D. Meiss, *Evolution of Magnetic Islands in a Heliac*; Sep. 1994

NIFS-309 H. Amo, T. Sato and A. Kageyama, *Intermittent Energy Bursts and Recurrent Topological Change of a Twisting Magnetic Flux Tube*; Sep.1994

NIFS-310 T. Yamagishi and H. Sanuki, *Effect of Anomalous Plasma Transport on Radial Electric Field in Torsatron/Heliotron*; Sep. 1994

NIFS-311 K. Watanabe, T. Sato and Y. Nakayama, *Current-profile Flattening and Hot Core Shift due to the Nonlinear Development of Resistive Kink Mode*; Oct. 1994

NIFS-312 M. Salimullah, B. Dasgupta, K. Watanabe and T. Sato, *Modification and Damping of Alfvén Waves in a Magnetized Dusty Plasma*; Oct. 1994

NIFS-313 K. Ida, Y. Miura, S -I. Itoh, J.V. Hofmann, A. Fukuyama, S. Hidekuma, H. Sanuki, H. Idei, H. Yamada, H. Iguchi, K. Itoh, *Physical Mechanism Determining the Radial Electric Field and its Radial Structure in a Toroidal Plasma*; Oct. 1994

NIFS-314 Shao-ping Zhu, R. Horiuchi, T. Sato and The Complexity Simulation Group, *Non-Taylor Magnetohydrodynamic Self-Organization*; Oct. 1994

NIFS-315 M. Tanaka, *Collisionless Magnetic Reconnection Associated with Coalescence of Flux Bundles*; Nov. 1994

NIFS-316 M. Tanaka,

Macro-EM Particle Simulation Method and A Study of Collisionless Magnetic Reconnection; Nov. 1994

NIFS-317 A. Fujisawa, H. Iguchi, M. Sasao and Y. Hamada,
Second Order Focusing Property of 210° Cylindrical Energy Analyzer; Nov. 1994

NIFS-318 T. Sato and Complexity Simulation Group,
Complexity in Plasma - A Grand View of Self- Organization; Nov. 1994

NIFS-319 Y. Todo, T. Sato, K. Watanabe, T.H. Watanabe and R. Horiuchi,
MHD-Vlasov Simulation of the Toroidal Alfvén Eigenmode; Nov. 1994

NIFS-320 A. Kageyama, T. Sato and The Complexity Simulation Group,
Computer Simulation of a Magnetohydrodynamic Dynamo II: Nov. 1994

NIFS-321 A. Bhattacharjee, T. Hayashi, C.C.Hegna, N. Nakajima and T. Sato,
Theory of Pressure-induced Islands and Self-healing in Three-dimensional Toroidal Magnetohydrodynamic Equilibria; Nov. 1994

NIFS-322 A. Iiyoshi, K. Yamazaki and the LHD Group,
Recent Studies of the Large Helical Device; Nov. 1994

NIFS-323 A. Iiyoshi and K. Yamazaki,
The Next Large Helical Devices; Nov. 1994

NIFS-324 V.D. Pustovitov
Quasisymmetry Equations for Conventional Stellarators; Nov. 1994

NIFS-325 A. Taniike, M. Sasao, Y. Hamada, J. Fujita, M. Wada,
The Energy Broadening Resulting from Electron Stripping Process of a Low Energy Au^- Beam; Dec. 1994

NIFS-326 I. Viniar and S. Sudo,
New Pellet Production and Acceleration Technologies for High Speed Pellet Injection System "HIPEL" in Large Helical Device; Dec. 1994

NIFS-327 Y. Hamada, A. Nishizawa, Y. Kawasumi, K. Kawahata, K. Itoh, A. Ejiri, K. Toi, K. Narihara, K. Sato, T. Seki, H. Iguchi, A. Fujisawa, K. Adachi, S. Hidekuma, S. Hirokura, K. Ida, M. Kojima, J. Koong, R. Kumazawa, H. Kuramoto, R. Liang, T. Minami, H. Sakakita, M. Sasao, K.N. Sato, T. Tsuzuki, J. Xu, I. Yamada, T. Watari,
Fast Potential Change in Sawteeth in JIPP T-IIU Tokamak Plasmas; Dec. 1994

NIFS-328 V.D. Pustovitov,
Effect of Satellite Helical Harmonics on the Stellarator Configuration; Dec. 1994